ISSN (Print) 1226-1750
ISSN (Online) 2233-6656
Journal of Magnetics 27(3), 256-262 (2022) https://doi.org/10.4283/JMAG.2022.27.3.256

A Fine Modified Calculation Model with Experimental Verification for the Holding Force of the Permanent Magnet

Peiliang Liu[1,2], Jigou Liu[1]*, and Ulrich Westenthanner[2]

[1]*R & D Department, ChenYang Technologies GmbH & Co. KG, Markt Schwabener Str. 8, 85464 Finsing, Germany*
[2]*Mechanical, Automotive, Aeronautical Engineering, Munich University of Applied Sciences, Lothstraße 64, 80335 Munich, Germany*

(Received 19 April 2022, Received in final form 14 July 2022, Accepted 20 July 2022)

For the common technical applications of permanent magnets such as cylindrical and rectangular permanent magnets, the formula of the holding force, which is based on the idea of equivalent current source and associated with Lorentz force, is fine modified with introducing two parameters, the chamfer size of the magnet and the thickness of the outer protective film. Furthermore, the model is verified by external experimental data. The accuracy of our proposed model has been significantly improved compared to the base model, with an average improvement of 6.3 %. With external data, the average error of the refined model is within 6 %. Compared to other currently available online calculators, our calculation model offers superior calculation accuracy.

Keywords : cylindrical permanent magnet, rectangular permanent magnet, analytical calculation, holding force, chamfer size, experimental verification

1. Introduction

Due to the ability to generate forces in a non-contact manner with excellent remanence, NdFeB permanent magnets are widely used as functional structures in industrial products, such as permanent lifting magnet [1], active magnetic refrigerator [2] and gripping devices in the robot arm [3]. For these products, the magnitude of the holding force, i.e., the force required to disengage the two permanent magnets in contact from each other, is a central design parameter. Thus, a method that allows the magnetic holding force to be calculated quickly and with reliable results has a significant impact on the overall product development cost.

However, in order to prevent oxidation, the outer surface of the NdFeB magnet is usually wrapped with a protective film [4], and for better electroplating results, NdFeB magnets also need to be chamfered before electroplating [5], this allows for slight differences between the actual structure and the ideal structure for typical magnet structures such as cylindrical or rectangular magnets. This also causing the measured holding force to deviate systematically from the calculated holding force. To the best of the authors' knowledge, a detailed exploration of the effects of these two parameters (chamfer size and thickness of the outer protective film) has not been addressed in the current.

In contrast to finite-element-method for which the intensity of discretization of the magnet geometry largely determines the accuracy of the calculation [6], the equivalent current-based method is still an effective way for the work in this paper because of its ability to calculate well for complex geometries [7].

In this paper, Section 2 describes the related work on the analytical calculation of magnetic forces, in Section 3 the analytical formula for cylindrical and rectangular permanent magnets are derived, in Section 4 the derived formula is verified experimentally, and the influence of the chamfer size and the thickness of the outer protective film is addressed. In Section 5, a conclusion is given.

2. Related Work

In the last decade, the formula for calculating the magnetic force between permanent magnets has been broadly studied, and it is a common practice to calculate the magnetic force as a function of the distance between two magnets. In [4] the calculation method of the magnetic force between cylindrical permanent magnets has been summarized and a new calculation method has been

*Corresponding author: Tel: +08121-2574114
Fax: +8121-2574110, e-mail: info@chenyang.de

proposed. However, according to its measurement with NdFeB magnet, the proposed calculation method is subject to a significant systematic error and one of the reasons it concludes is the presence of the outer protective film.

An approximate calculation method [8] of magnetic force between two cylindrical magnets has also been used to simplify the calculation by dividing the entire cylindrical magnet into small cubes, the accuracy can be controlled by the number of cubes.

In the paper [7], the accuracy of the equivalent current-based method and the Equivalent Magnetic Charge method for calculating the magnetic force between rectangular and cylindrical permanent magnets is compared, and the NdFeB magnets are still used as experimental materials.

However, all of the above-mentioned methods for magnetic force calculations do not take into account the presence of chamfers and consider the permanent magnet simply as an ideally regular geometry.

The effect of the size of the chamfer and the thickness of the outer protective film on the accuracy of the calculation model will be considered in detail in this paper.

3. Model Derivation

3.1. Derivation of the current element

According to Ampere's law, the magnetic force dF derived from a current element $Id\vec{l}$ in an external magnetic field with a magnetic induction of $\vec{B}$ is:

$$dF = Id\vec{l} \times \vec{B} \tag{1}$$

It is assumed in this work the permanent magnet is uniformly magnetized. Then the average surface current density $\vec{J}_m$:

$$\vec{J}_m = \vec{M}_r \times \hat{n} \tag{2}$$

Where $\hat{n}$ is the unit normal vector on the surface of the permanent magnet, $\vec{M}_r$ is the magnetization intensity of the permanent magnet.

Because the influence is small, the change of the magnetization intensity of the permanent magnet due to the presence of the external magnetic field is neglected.

According to (2), the average surface current density exists only on the side surface of the magnet and the quantity is also the magnetization intensity, i.e., $J_m = M_r = B_r/\mu_0$, B_r is the remanence of the magnet and μ_0 is the vacuum permeability.

In this paper, we discretize the outer surface of the magnet in the circumferential as well as the radial direction to obtain the current source $Id\vec{l}$.

As showed in Fig. 1, a current element has an intensity

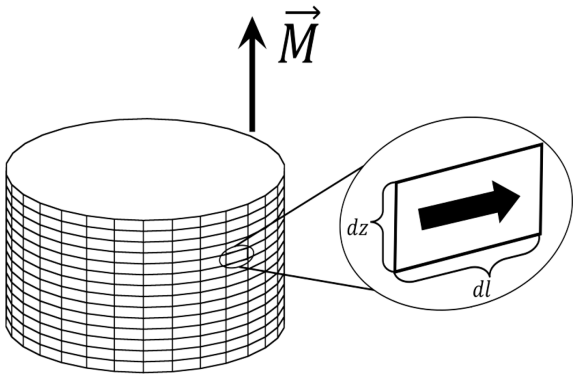

Fig. 1. Diagram of the general equivalent current model.

$I = \frac{B_r}{\mu_0} dz$, a length of dl, and the thickness of dz. The direction of the current source is tangential to the outer surface of the magnet, and perpendicular to the direction of magnetization.

Thus, formula (1) can be rewritten as follows:

$$dF = \frac{B_r d\vec{l} \times \vec{B}}{\mu_0} dz \tag{3}$$

3.2. Holding force between cylindrical permanent magnets

The arrangement of two coaxial cylindrical permanent magnets is shown in Fig. 2:

A coordinate system is established as shown in Fig. 2, with the origin O of the coordinates at the center of the lower surface of the bottom magnet and, for ease of representation, the angle θ is noted as the angle between the plane XOZ and the plane POZ.

In practice, NdFeB permanent magnets have a chamfer

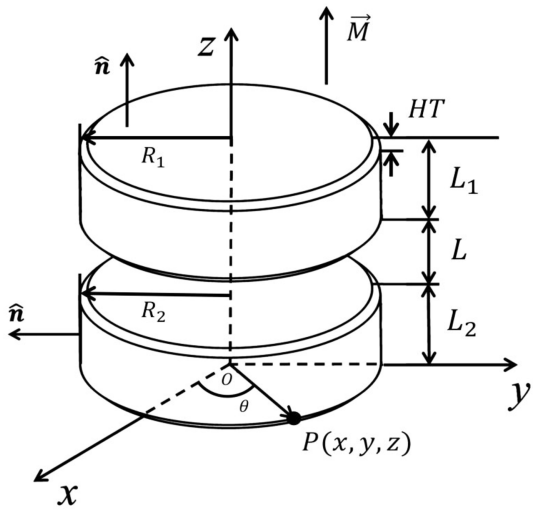

Fig. 2. Two coaxial cylindrical permanent magnets.

as well as a protective film, so in the calculation model presented in this paper, the variables *HT* and *L* are introduced, and furthermore, the chamfer is considered as a 45 chamfer in this paper.

According to equation (3), the magnetic force *F* between two ideal cylindrical magnets:

$$F = \frac{1}{\mu_0} \int_{L2+L}^{L+L1+L2} \int_0^{2\pi} B_r d\vec{l} \times \vec{B} d\theta dz \tag{4}$$

where $d\vec{l} = (-R_1 \sin\theta d\theta, R_1 \cos\theta, 0)$.

At the meantime, the magnetic field strength at an arbitrary coordinate $\vec{B}$ can be described by the following formula:

$$\vec{B} = \vec{B}_o + \vec{B}_u \tag{5}$$

$\vec{B}_o$ is the magnetic field excited by the upper cylindrical permanent magnet and $\vec{B}_u$ for the lower permanent magnet. $\vec{B}_o$ is symmetrical about the middle section of the upper cylindrical magnet, therefore the integral result of $\vec{B}_o$ in the equation (4) is 0, thus formula (4) can be simplified:

$$F = \frac{1}{\mu_0} \int_{L2+L}^{L+L1+L2} \int_0^{2\pi} B_r d\vec{l} \times \vec{B}_u d\theta dz \tag{6}$$

Next, the formula for the spatial magnetic field strength distribution is needed. Based on the idea of the equivalent current source, the formula for cylindrical permanent magnets [9] is:

$$B_x = \frac{\mu_0 J_m}{4\pi} \int_0^h \int_0^{2\pi} \frac{r_0 (z - z_0) \cos\theta}{K} d\theta dz_0 \tag{7}$$

$$B_y = \frac{\mu_0 J_m}{4\pi} \int_0^h \int_0^{2\pi} \frac{r_0 (z - z_0) \sin\theta}{K} d\theta dz_0 \tag{8}$$

where $K = [(x - r_0 \cos\theta)^2 + (y - r_0 \sin\theta)^2 + (z - z_0)^2]^{1.5}$, and r_0 is the radius and h is the thickness of the cylindrical permanent magnet.

Now, the magnetic force between two ideal cylindrical magnets can be calculated by bringing B_x and B_y into equation (6). At this point, the term $d\vec{l} \times \vec{B}_u$ in equation (6) can be written in the following form:

$$d\vec{l} \times \vec{B}_u = \begin{vmatrix} x & y & z \\ -R_1 \sin\theta d\theta & R_1 \sin\theta d\theta & 0 \\ B_x & B_y & B_z \end{vmatrix} \tag{9}$$

Since the magnetic field generated by a cylindrical permanent magnet has symmetry around its central axis, the term $d\vec{l} \times \vec{B}_u$ is the same for any value of θ, so this paper only considers the case when $\theta = 0$. That is, only the value of this term at the point $(R_1, 0, z)$ needs to be calculated:

$$d\vec{l} \times \vec{B}_u = -R_1 B_x(R_1, 0, z) \tag{10}$$

From there, equation (6) can be further simplified to

$$F = -\frac{2\pi B_r}{\mu_0} \int_{L2+L}^{L+L1+L2} R_1 B_x(R_1, 0, z) dz \tag{11}$$

Taking equation (7) into equation (11), the final equation of magnetic force between two ideal cylindrical magnets is

$$F_{CA0} = -\frac{B_r^2}{2\mu_0} \int_{L2+L}^{L1+L2+L} \int_0^{L2} \int_0^{2\pi} \frac{R_1 R_2 (z - z_0) \cos\theta}{[(R_1 - R_2 \cos\theta)^2 + (R_2 \sin\theta)^2 + (z - z_0)^2]^{1.5}} d\theta dz_0 dz \tag{12}$$

To account for the chamfer, the chamfered cylindrical magnet can be divided into three parts: the upper circular table structure, the lower circular table structure, and the middle cylindrical structure. In this way, the magnetic force of the chamfered cylindrical magnet consists of nine parts, as shown in Fig. 3.

In Fig. 3, the areas indicated in gray in each small diagram represent the force-generating and force-receiving parts of the structure, where the lower structure is the force-generating part of the chamfered magnet and the upper structure represents the force-receiving part. For ease of representation, the corresponding cases are represented by the numbers in the lower right corner of each small diagram.

Ultimately, by modifying equation (12) the holding force between two coaxially placed chamfered cylindrical permanent magnets F_{CB} can be calculated by the following

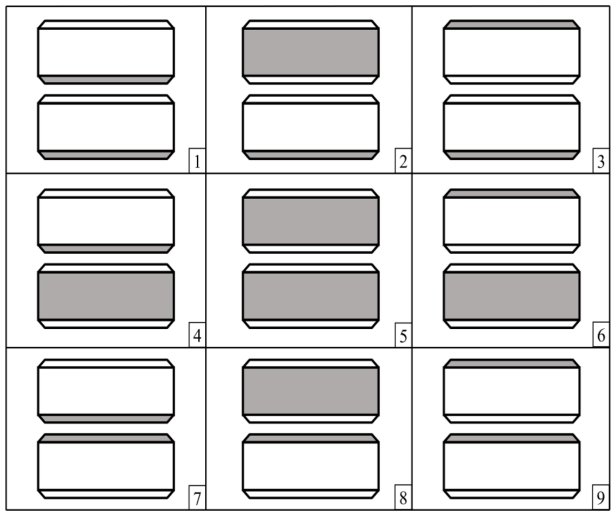

Fig. 3. Diagram of the composition of the magnetic force between two chamfered cylindrical magnets.

equation:

$$F_{CB} = F_{CB1} + F_{CB2} + F_{CB3} \tag{13}$$

$$F_{CB1} = -\frac{B_r^{\,2}}{2\mu_0}\left(\int_{L_2+L}^{HT+L_2+L} A_{x1}dz + \int_{HT+L_2+L}^{L_1+L_2+L-HT} A_{x2}dz + \int_{L_1+L_2+L-HT}^{L_1+L_2+L} A_{x3}dz \right) \tag{14}$$

$$F_{CB2} = -\frac{B_r^{\,2}}{2\mu_0}\left(\int_{L_2+L}^{HT+L_2+L} A_{x4}dz + \int_{HT+L_2+L}^{L_1+L_2+L-HT} A_{x5}dz + \int_{L_1+L_2+L-HT}^{L_1+L_2+L} A_{x6}dz \right) \tag{15}$$

$$F_{CB3} = -\frac{B_r^{\,2}}{2\mu_0}\left(\int_{L_2+L}^{HT+L_2+L} A_{x7}dz + \int_{HT+L_2+L}^{L_2+L_1+L-HT} A_{x8}dz + \int_{L_2+L_1+L-HT}^{L_2+L_1+L} A_{x9}dz \right) \tag{16}$$

where

$$A_{xj} = \int_{ZA}^{ZB}\int_{0}^{2\pi} \frac{R_{2j}R_{1j}\left(z-z_0\right)\cos\theta}{\left[\left(x_j - R_{2j}\cos\theta\right)^2 + \left(y_j - R_{2j}\sin\theta\right)^2 + \left(z-z_0\right)^2\right]^{1.5}} d\theta dz \tag{17}$$

The parameters $\left[R_{2j}, x_j, y_j, R_{1j}, ZA, ZB\right]$ in the expression A_{xj} are replaced line by line by the expressions in the matrix. The matrix is a two-dimensional matrix, and each row of the matrix represents the magnetic force between different cylindrical magnet parts, and there are nine rows corresponding to the nine parts of the magnetic force. The parameters contained in the jth row of the matrix correspond to the magnetic parts with the same number in Fig. 3.

$$\left[R_{1j}, x_j, y_j, R_{2j}, ZA, ZB\right] =$$
$$\begin{bmatrix}
R_1-HT+(z-L_2-L), R_1-HT+(z-L_2-L), 0, R_2-HT+z_0, 0, HT \\
R_1, R_1, 0, R_2-HT+z_0, 0, HT \\
R_1-(z-L_1-L-L_2+HT), R_1-(z-L_1-L-L_2+HT), 0, R_2-HT+z_0, 0, HT \\
R_1-HT+(z-L_2-L), R_1-HT+(z-L_2-L), 0, R_2, HT, L_2-HT \\
R_1, R_1, 0, R_2, HT, L_2-HT \\
R_1-(z-L_1-L-L_2+HT), R_1-(z-L_1-L-L_2+HT), 0, R_2, HT, L_2-HT \\
R_1-HT+(z-L_2-L), R_1-HT+(z-L_2-L), 0, R_2-(z_0-L_2+HT), L_2-HT, L_2 \\
R_1, R_1, 0, R_2-(z_0-L_2+HT), L_2-HT, L_2 \\
R_1-(z-L_1-L-L_2+HT), R_1-(z-L_1-L-L_2+HT), 0, R_2-(z_0-L_2+HT), L_2-HT, L_2
\end{bmatrix}$$

3.3. Holding force between rectangular permanent magnets

Similarly, two rectangular permanent magnets placed coaxially are shown in the Fig. 4 below.

It is worth noting that the chamfers on the four sides of the rectangular permanent magnets are not considered in this model, because the magnetic material near the contact surface of the two magnets contributes significantly to the overall magnetic force, while the other areas contribute relatively little, and also in order not to make the model too complicated.

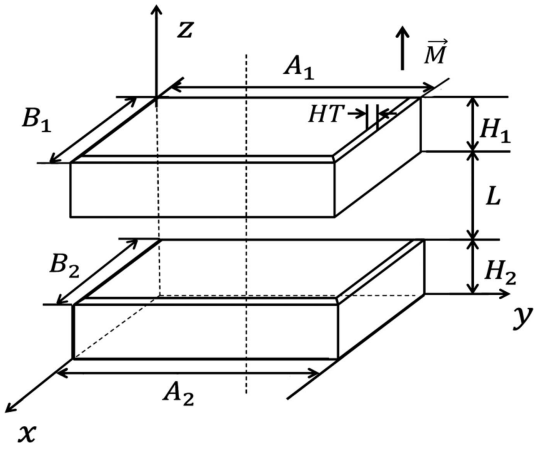

Fig. 4. Two coaxial rectangular permanent magnets.

According to [10], the formulas for the magnetic field strength of ideal rectangular permanent magnets in the x, y direction are:

$$B_x(x,y,z) = -\frac{K}{2}\left[\Gamma(a-x,y,z) + \Gamma(a-x,b-y,z) - \Gamma(x,y,z) - \Gamma(x,b-y,z)\right]\Big|_0^h \tag{18}$$

$$B_y(x,y,z) = -\frac{K}{2}\left[\Gamma(b-x,y,z) + \Gamma(b-y,a-x,z) - \Gamma(y,x,z) - \Gamma(y,a-x,z)\right]\Big|_0^h \tag{19}$$

where $K = \mu_0 J_m / 4\pi$, and

$$\Gamma(\gamma_1,\gamma_2,\gamma_3) = \ln\frac{\sqrt{\gamma_1^2+\gamma_2^2+\left(\gamma_3-z_0\right)^2}-\gamma_2}{\sqrt{\gamma_1^2+\gamma_2^2+\left(\gamma_3-z_0\right)^2}+\gamma_2} \tag{20}$$

$[\phi]\big|_0^h$ means the difference in value of the function ϕ at $z_0 = h$ and $z_0 = 0$, where h is thickness of the rectangular magnet, a and b imply the length and width of the rectangular.

For the chamfered rectangular magnets, we notate the function $A(a,b,h,x,y,z)$:

$$\begin{aligned}
&A(a,b,h,x,y,z) = \\
&B(a,b,h-2HT,x,y,z-HT) \\
&+\sum_{n=0}^{m} B\left(a-\frac{2nHT}{m}, b-\frac{2nHT}{m}, \frac{HT}{m}, x-\frac{nHT}{m}, y-\frac{nHT}{m}, z-\frac{nHT}{m}-h_1+HT\right) \\
&+\sum_{n=0}^{m} B\left(a-\frac{2nHT}{m}, b-\frac{2nHT}{m}, \frac{HT}{m}, x-\frac{nHT}{m}, y-\frac{nHT}{m}, z-\frac{nHT}{m}\right)
\end{aligned} \tag{21}$$

By dividing the top and bottom chamfered part into m ideal thin rectangular magnets, the function $A(a,b,h,x,y,z)$ calculates the magnetic field strength generated by the chamfered rectangular magnet at space (x,y,z). Function $A(a,b,h,x,y,z)$ is valid for both x,y directions, when

the function B_x is brought into the function $A(a,b,h,x,y,z)$, the calculated magnetic field strength is in x direction. Based on experience, m is chosen to be 1e4.

Since the magnetic field of the chamfered rectangular magnet can be calculated directly by the function $A(a,b,h,x,y,z)$, the magnetic force between two chamfered rectangular magnets is composed of three parts, namely the force generated by the chamfered part below, by the chamfered part above and by the rectangular part in the middle.

Finally, the formula for calculating the holding force F_{BB} between two coaxial placed and chamfered rectangular permanent magnets is:

$$F_{BB}=\frac{-4B_r}{\mu_0}\left[\begin{array}{l}\int_{H_2+L}^{H_2+L+HT}\int_{\frac{A_2}{2}}^{\frac{A_2}{2}+\frac{A_1}{2}+\alpha}A_{xu}\left(a1,b1,h1,\frac{B_1+B_2}{2}+\alpha,y,z\right)dydz+\\ \int_{H_2+L}^{H_2+L+HT}\int_{\frac{B_2}{2}}^{\frac{B_2}{2}+\frac{B_1}{2}+\alpha}A_{yu}\left(a1,b1,h1,x,\frac{A_1+A_2}{2}+\alpha,z\right)dxdz\end{array}\right]+$$
$$\frac{-4B_r}{\mu_0}\left[\begin{array}{l}\int_{H_2+L+HT}^{H_1+H_2+L-HT}\int_{\frac{A_2}{2}}^{\frac{A_2}{2}+\frac{A_1}{2}}A_{xu}\left(a1,b1,h1,\frac{B_1+B_2}{2},y,z\right)dydz+\\ \int_{H_2+L+HT}^{H_1+H_2+L-HT}\int_{\frac{B_2}{2}}^{\frac{B_2}{2}+\frac{B_1}{2}}A_{yu}\left(a1,b1,h1,x,\frac{A_1+A_2}{2},z\right)dxdz\end{array}\right]+ \quad (22)$$
$$\frac{-4B_r}{\mu_0}\left[\begin{array}{l}\int_{H_1+H_2+L-HT}^{H_1+H_2+L}\int_{\frac{A_2}{2}}^{\frac{A_2}{2}+\frac{A_1}{2}+\beta}A_{xu}\left(a1,b1,h1,\frac{B_1+B_2}{2}+\beta,y,z\right)dydz+\\ \int_{H_1+H_2+L-HT}^{H_1+H_2+L}\int_{\frac{B_2}{2}}^{\frac{B_2}{2}+\frac{B_1}{2}+\beta}A_{yu}\left(a1,b1,h1,x,\frac{A_1+A_2}{2}+\beta,z\right)dxdz\end{array}\right]$$

Where $\alpha=-HT+(z-H_2-L)$ and $\beta=-(z-H_1-L-H_2+HT)$.

B_{xu} and B_{yu} mean the magnetic flux density generated by the lower permanent magnet.

Similarly, the formula of the comparison method is as follows:

$$F_{BA0}=\frac{-4B_r}{\mu_0}\left[\begin{array}{l}\int_{H_1}^{H_1+H_2}\int_{\frac{A_2}{2}}^{\frac{A_2}{2}+\frac{A_1}{2}}B_{xu}\left(a,b,h,\frac{B_1+B_2}{2},y,z\right)dydz+\\ \int_{H_1}^{H_1+H_2}\int_{\frac{B_2}{2}}^{\frac{B_2}{2}+\frac{B_1}{2}}B_{yu}\left(a,b,h,x,\frac{A_1+A_2}{2},z\right)dxdz\end{array}\right] \quad (23)$$

B_{xu} and B_{yu} mean the magnetic field strength generated by the lower permanent magnet.

4. Model Verification

The thickness of the protective film of permanent magnets is usually 0.02 mm, the distance between two magnets is chosen to be 0.05 mm. This distance is comparable to the thickness of the protective layer measured in the work of [4]. The size of the chamfer is heuristically chosen to be 0.5 mm. The calculation model is implemented in Matlab 2019b platform, the integration operator is implemented by the function '*integral2*' and the parameter '*AbsTol*' is chosen as 1e-3, which means that the absolute error of integration is less than 1e-3.

To study the influence of these two geometrical parameters, four forms of parameter combinations have been selected to form four calculation models in this paper, as shown in the following Table 1.

To verify the accuracy of the model, the calculated results were compared with external experimental magnetic force data provided by [11]. The digital force gauge *Mark-10* records the force on the magnet. The permanent magnets are pulled apart until the magnet is disconnected and the peak is recorded. The values are an average value for five samples of each magnet.

The remanence of the NdFeB magnet is 1.24 T. Since the data provided were obtained experimentally, the distance between the two magnets is chosen to be 0 mm. In total, six pairs of cylindrical permanent magnets were selected, with typical dimensions of ∅15×20, ∅20×5, ∅20×10, ∅20×20, ∅30×10 and ∅30×20, eight pairs of rectangular permanent magnets were selected, with typical dimensions of 10×10×5, 15×10×5, 15×15×5, 15×15×10, 15×15×15, 20×10×5, 30×10×10 and 40×30×20. The units of these numbers are all in mm.

Also, in this paper, we compare the calculation accuracy of current online calculators from other companies. The online calculator for the magnetic force between two cylindrical magnets is available from Supermagnete [12]. The selected magnet was NdFeB magnet N38 with remanence between 1.22 T and 1.26 T, and the contact distance between the magnets was chosen as 0 mm according to the company's requirements. Calculation of the magnetic force between two rectangular magnets was

Table 1. Composition of the parameters of the four models and their names.

Model name	Chamfer size HT	Protective film thickness L
model-A0	0 mm	0 mm
model-AC	0.5 mm	0 mm
model-AF	0 mm	0.05 mm
model-B	0.5 mm	0.05 mm

Table 2. Magnetic force measurements of two identical and coaxial cylindrical permanent magnets and the calculated relative errors of four models, experimental data provided by [11].

Dimension mm	∅15×20	∅20×5	∅20×10	∅20×20	∅30×10	∅30×20
exp. results N	91.4	69.3	108.4	146	190.1	283.3
model-A0 N	97.2	74.6	120.9	161.8	209.2	314.7
relative error	6.3 %	7.6 %	11.5 %	10.8 %	10.0 %	11.1 %
model-AC N	95.1	71.8	118.1	158.9	205.1	310.5
relative error	4.0 %	3.6 %	8.9 %	8.8 %	7.9 %	9.6 %
model-AF N	94.5	71.5	117.4	158.0	204.0	308.8
relative error	3.4 %	3.2 %	8.3 %	8.2 %	7.3 %	9.0 %
model-B N	92.4	69.0	114.8	155.4	200.4	305.2
relative error	1.1 %	0.4 %	5.9 %	6.8 %	5.4 %	7.7 %
Supermagnete	79.2	58.1	96.5	131.5	165.3	254.3
relative error	13.3 %	16.2 %	11.0 %	7.9 %	13.0 %	10.2 %

Table 3. Magnetic force measurements of two identical and coaxial rectangular permanent magnets and the calculated relative errors of the four models, experimental data provided by [11].

Dimension mm	10×10×5	15×10×5	15×15×5	15×15×10	15×15×15	20×10×5	30×10×10	40×30×20
exp. results N	31.7	43.1	56.6	86.5	102.4	53.1	103.8	415.2
model-A0 N	36.3	48.6	62.4	95.3	112	60.5	126	474.9
relative error	14.5 %	12.8 %	10.2 %	10.2 %	9.4 %	13.9 %	21.4 %	14.4 %
model-AC N	30.9	41.4	53.8	85.3	101.4	51.4	113.4	449.0
relative error	2.5 %	3.9 %	4.9 %	1.4 %	1.0 %	3.2 %	9.2 %	8.1 %
model-AF N	34.4	46.2	59.6	92.1	108.7	57.6	121.7	466.5
relative error	8.5 %	7.2 %	5.3 %	6.5 %	6.2 %	8.5 %	17.2 %	12.4 %
model-B N	29.7	40.2	52.3	83.7	99.5	49.8	111.0	443.9
relative error	6.7 %	6.7 %	7.6 %	3.2 %	2.8 %	6.2 %	6.9 %	6.9 %
Int. Magnetics	49.4	106.8	236.7	54.7	16.5	168.6	78.3	414.1
relative error	55.8 %	147.8 %	318.2 %	36.8 %	83.9 %	217.5 %	24.6 %	0.3 %

provided by Integrated Magnetics [13] and the remanence of magnets was chosen as 1.24T. The distance between magnets is chosen to be 0 mm, because if the distance is chosen to be 0.05 mm, the data error is ridiculously large.

The calculated results and Corresponding errors are shown in Tables 2 and 3.

Ultimately, the mean errors for the four models with other online calculators are shown in the Table 4.

According to the experimental results, for the magnetic holding force between cylindrical magnets, the accuracy of model-B is better than any other models, and the calculation accuracy of model-A0 is the worst, while the accuracy of model-AF is slightly better than that of model-AC, but still lower than the accuracy of model-B. Compared to the online calculator provided by Supermagnete, model-B still provides significantly more accurate results.

Table 4. Mean error of the four models.

Model	Mean error in cylindrical permanent magnets by [11]	Mean error in rectangular permanent magnets by [11]
model-A0	9.6 %	13.4 %
model-AC	7.1 %	4.3 %
model-AF	6.6 %	9.0 %
model-B	4.6 %	5.9 %
Supermagnete	11.93 %	/
Int. Magnetics	/	110.6 %

For rectangular magnets, the accuracy of model-AC is best at smaller sizes, and for larger sizes model-B is more accurate, while model-B still maintains a high accuracy at smaller sizes, with an average accuracy of 5.9 %. Similarly, the model-A0 algorithm has the worst accuracy. It is worth noting that the online magnetic force calculator by Int. Magnetics provides almost no valid results for most of the selected dimensions, while model-B provides more accurate results for all dimensions.

It is also necessary to compare the increase in computation time to evaluate its suitability for application as an online calculator. In Table 5 the average times for calculating cylindrical permanent magnets as well as

Table 5. Average calculation time for model-A0 and model-B.

Model	Average calculation time for cylindrical permanent magnets	Average calculation time for rectangular permanent magnets
model-A0	0.142 s	0.005 s
model-B	0.456 s	0.580 s

rectangular permanent magnets are presented for model-B and model-A0, respectively.

In this paper, for each cylindrical or rectangular magnet size the measurements of calculation time are repeated five times and then averaged. After that, the calculation times of all sizes of cylindrical or rectangular permanent magnets are averaged again, and the average calculation time is finally obtained. The computing core is Intel Core i5-6300HQ.

In summary, the results of model-B are significantly better than those of model-A0 without considering these two factors, even for a heuristic selection of values of chamfer size. For the database provided by [11], the average accuracy of model-B reaches within 6 %. However, the computation time of model-B increases significantly compared to the base model, with each computation time around 0.5 s.

5. Conclusion

In this paper, the equation for calculating the magnetic holding force is fine considered, and two parameters, the chamfer size of the magnet and the thickness of the outer protective film of the magnet, are introduced in the model.

It was broadly verified that both parameters have a large effect on the accuracy of the model. Collectively, model-B (models with consideration of chamfers and protective film) achieves a significant improvement in accuracy compared to other models, with an average of 6.3 % improvement compared to the basic model-A0 (models without consideration of chamfers and protective film). According to external experimental data [11], the overall average accuracy of model-B is within 6 %, which also demonstrates the transferability and reliability of the performance of this model. Compared to other online calculators, model-B provides superior calculations within the selected magnet size. However, attention also needs to be paid to the computational intensity caused by the introduction of the two parameters.

References

[1] Online shop for permanent lifting magnet, https://www.jh-profishop.de/Dolezych-Permanent-Lasthebemagnet-586906-280624/, at time 2022/3/19
[2] Z. G. Zheng, H. Y. Yu, X. C. Zhong, D. C. Zeng, and Z. W. Liu, Int. J. Refrig. **32**, 78 (2009).
[3] C. C. Chen, T. K. Chung, and C. Y. Lin, IEEE Trans. Magn. **53**, 1 (2017).
[4] D. Vokoun, G. Tomassetti, M. Beleggia, and I. Stachiv, J. Magn. Magn. Mater. **323**, 55 (2011).
[5] X. G. Bai and G. H. Pan, Method for chamfering permanent magnet material, China Patent No. 101722449B.
[6] K. J. Meessen, J. J. H. Paulides, and E. A. Lomonova, IEEE Trans. Magn. **49**, 536 (2013).
[7] Y. Y. Zhang, Y. G. Leng, J. J. Liu, and D. Tan, J. Magnetics **24**, 392 (2019).
[8] N. Mohdeb, H. Allag, and T. Hacib, Prog. Electromagn. Res. C **91**, 213 (2019).
[9] E. Q. Zhou, Z. Q. Zheng, Y. H. Zhang, and Q. R. Wang, Journal of Henan Science and Technology **42**, 140 (2017).
[10] X. F. Gou, Y. Yang, and X. J. Zheng, J. Appl. Math. Mech. (Engl. Transl.) **25**, 297 (2004).
[11] Experimental magnetic force data, https://www.kjmagnetics.com/calculator.asp, at time 2022/3/14
[12] Magnetic force online-calculator from Supermagnete, https://www.supermagnete.de/eng/adhesive-force-calculation/, at time 2022/3/21
[13] Magnetic force online-calculator from Integrated Magnetics, https://www.intemag.com/magnet-push-or-pull-calculations-between-rectangular-magnets, at time 2022/3/21